Optical Materials 88 (2019) 424–428

Contents lists available at ScienceDirect

Optical Materials

journal homepage: www.elsevier.com/locate/optmat

Fabrication and characterization of ZnS:Ag-based ultrafiltration membrane scintillator

Y. Wu[a], A.W. Darge[b], A.A. Trofimov[a], C. Li[a], K.S. Brinkman[a], S.M. Husson[b], L.G. Jacobsohn[a,c,*]

[a] Department of Materials Science and Engineering, Clemson University, Clemson, SC, 29634, USA
[b] Department of Chemical and Biomolecular Engineering, Clemson University, Clemson, SC, 29634, USA
[c] School of Chemistry and Pharmaceutical Engineering, Taishan Medical University, Taian, 271016, PR China

ARTICLE INFO

Keywords:
ZnS:Ag
Solid state reaction
Scintillator
Ultrafiltration membrane
Special nuclear material

ABSTRACT

This contribution describes the fabrication of an ultrafiltration membrane scintillator based on ZnS:Ag. A solid state reaction method was used for the synthesis of ZnS:Ag, with particular emphasis on investigating the effects of the reaction temperature on the ZnS host, and of the Ag concentration on the radioluminescence (RL) output. The reaction temperature was found to control the crystallite size between 3 and 10 nm for temperatures between 75 and 500 °C, while the RL output was maximized for an Ag concentration of 0.2 mol%. Modified membranes were coated with ZnS:Ag powders via ultrafiltration and their response to ionizing radiation was characterized by means of RL measurements.

1. Introduction

The overarching goal of this research is the development of a reactive ultrafiltration membrane scintillator for rapid activity determination and isotopic quantification of waterborne special nuclear materials (SNM). Reactive ultrafiltration membranes with uranium selective ligands have been prepared that enable the rapid isolation and concentration of SNM from aqueous solutions [1]. The addition of ZnS:Ag nanoparticles to a reactive ultrafiltration membrane is proposed as a fast and reliable method to conduct forensics of debris from a nuclear event.

The proposed rapid activity quantification of SNM is based on the detection and measurement of the alpha radiation emitted from uranium and plutonium. ZnS:Ag is the most efficient scintillator for alpha particle radiation. Its high luminosity of 60,000 photons/MeV, fast decay time of ~0.2 ms, and non-hygroscopic nature [2,3] make this scintillator the ideal choice for this application. The objective is to combine the high efficiency of ZnS:Ag scintillation with the rapid, selective concentration of SNM afforded by ultrafiltration to generate the maximum scintillation signal to optimize detection, enhance sensitivity for the radioactive isotopes, and decrease measurement time. Within this framework, our work focused on the synthesis, microstructure and luminescence characterization of ZnS:Ag prepared by solid state reaction, and the fabrication of a ZnS:Ag-based ultrafiltration membrane scintillator.

2. Experimental procedure

Undoped and Ag-doped ZnS were synthesized by means of solid state reaction. Zinc acetate (Alfa Aesar, 99.9 + %, anhydrous), thioacetamide (Alfa Aesar, 99%, ACS reagent), and silver nitrate ACS (Alfa Aesar, > 99.9%) were used as starting materials. The starting materials were dispersed in deionized water to facilitate ball milling. For undoped samples, the molar ratio of zinc acetate to thioacetamide was 1:1. For Ag-doped samples, the amount of silver nitrate was adjusted to achieve from 0.05 to 3 mol% substitution of Zn keeping the reaction temperature at 500 °C and the amount of thioacetamide fixed. The precursor solution was ball milled with zirconia balls for 48 h, followed by drying at 60 °C for 48 h. The residual powder was thoroughly ground using an agate mortar and pestle, and heated in a programmable tube furnace at temperatures from 75 to 500 °C for 5 h in air.

Membrane scintillators were fabricated using EMD Millipore Corporation PBHK04310 polyether sulfone (PES) ultrafiltration membranes (44.5 mm diameter, 100 kDa nominal molecular weight cutoff (MWCO) [4]). The surface of the membranes was modified with ethylene glycol methacrylate phosphate (EGMP, SNM-binding ligand) via ultraviolet initiated radical polymerization. The details of the surface modification have been published elsewhere [1]. The energy of the alpha particles from the targeted actinides is approximately 5 MeV which corresponds to a range of about 20 μm in ZnS, according to range calculations using the computer code SRIM 2013 [5]. As such, the

* Corresponding author. Department of Materials Science and Engineering, Clemson University, Clemson, SC, 29634, USA.
E-mail address: luiz@clemson.edu (L.G. Jacobsohn).

https://doi.org/10.1016/j.optmat.2018.12.009
Received 23 October 2018; Accepted 2 December 2018

modified ultrafiltration membrane was coated with a nominal 20 μm thick ZnS:Ag layer via filtration of a ZnS:Ag solution prepared by dispersing 100 mg ZnS:Ag in 20 mL deionized distilled water (DDI).

Imaging was conducted by scanning electron microscopy (SEM) using a Hitachi S3400 variable pressure electron microscope operated at 20 kV, and also by transmission electron microscopy (TEM) using a Hitachi H7600 operated at 120 kV. Optical microscopy was executed using a Horiba LabRAM HR Evolution microscope with a 5x magnification eyepiece.

X-ray diffraction (XRD) was conducted using a Rigaku AFC-7R (18 kW) diffractometer using CuKα radiation with 1°/min scanning rate.

Radioluminescence (RL) measurements were performed using a customer-designed Freiberg Instruments Lexsyg Research spectrofluorometer equipped with a Varian Medical Systems VF-50J X-ray tube with a tungsten target coupled with an ionization chamber for dose measurement. The light emitted by the sample was collected by a lens and converged into an optical fiber connected to an Andor Technology Shamrock 163 spectrograph coupled to an Andor Technology DU920P-BU Newton CCD camera. RL measurements were executed under continuous X-ray irradiation (40 kV and 1 mA) at room temperature. Powders filled *ca.* 8 mm diameter 1 mm deep cups thus allowing for relative RL intensity comparison among different samples. Results were not corrected for the spectral sensitivity of the system.

3. Results and discussion

The morphology of the powders is illustrated in the images shown in Fig. 1 obtained by SEM measurements in backscattered electron mode (Fig. 1A) and secondary electron mode (Fig. 1B). The powders were composed of irregular grains with a broad range of sizes, sometimes agglomerating to form large particles. The reaction temperature did not appear to significantly impact size and morphology of the grains. Fig. 2 shows the XRD results obtained from powders prepared at different solid state reaction temperatures, together with two powder diffraction files for the cubic (01-071-5975; red) and hexagonal (00-010-0434; blue) phases of ZnS. The results showed the solid state reaction powders to be single phase with the cubic crystallographic arrangement, as confirmed by the absence of the diffraction peaks (102) and (103) of the hexagonal phase. As the reaction temperature increased, diffraction peaks narrowed and the presence of lower intensity cubic diffraction peak (200) became more evident. The narrowing of the diffraction peaks was related to the increase of the average crystallite size, which was calculated applying Debye's formula [6] to diffraction peaks (111), (220) and (311). Fig. 3 shows the average crystallite size and corresponding standard deviation as a function of the reaction temperature. Crystallite sizes ranged from 3 to 10 nm, overall increasing for higher reaction temperatures as shown by the linear best fit (dotted line), in agreement with previous works [7,8]. The nanocrystalline nature of the powders was further confirmed by TEM measurements illustrated in Fig. 4.

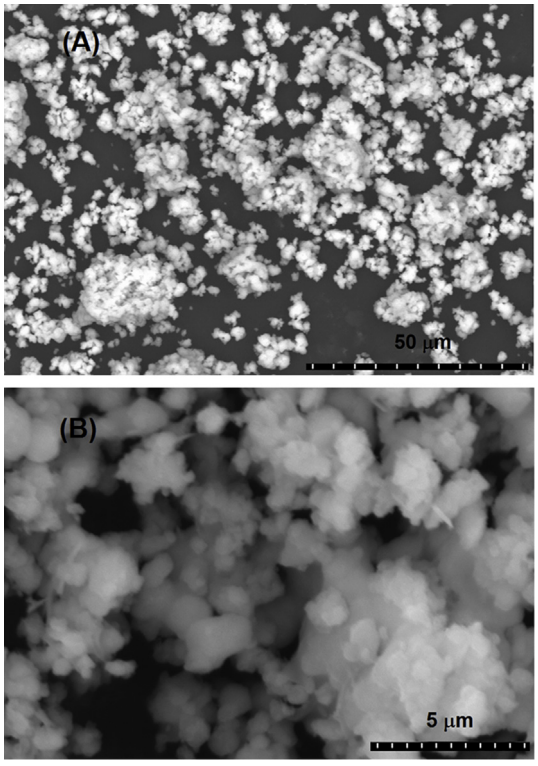

Fig. 1. SEM images of powders prepared by the solid state reaction method at 500 °C obtained in (A) backscattered electron mode, and (B) secondary electron mode, at different magnifications.

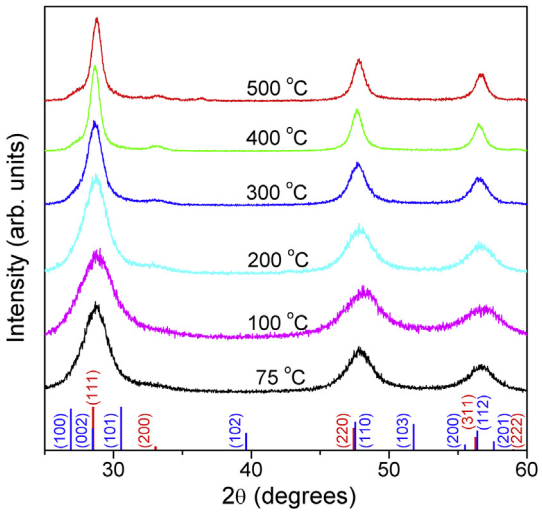

Fig. 2. X-ray diffractograms of ZnS powders prepared by the solid state reaction method at different reaction temperatures. The diffractograms were shifted vertically to improve clarity. The powder diffraction files for the cubic (01-071-5975; red bars) and hexagonal (00-010-0434; blue bars) phases of ZnS are also shown. (For interpretation of the references to colour in this figure legend, the reader is referred to the Web version of this article.)

The effect of the solid state reaction temperature on the luminescence response of the undoped ZnS host was investigated by RL measurements. Fig. 5A shows typical RL spectra obtained from powders

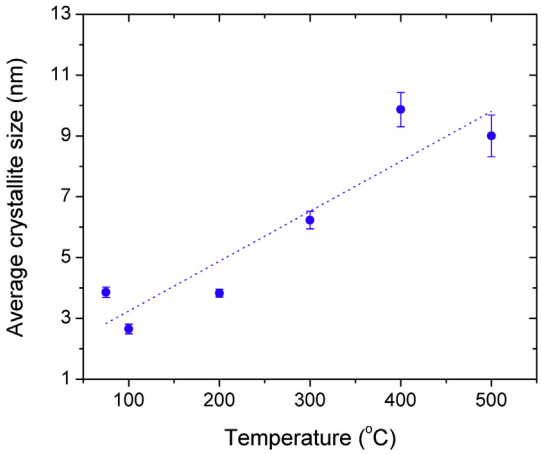

Fig. 3. Average crystallite size as a function of the solid state reaction temperature, together with linear best fit (dotted line).

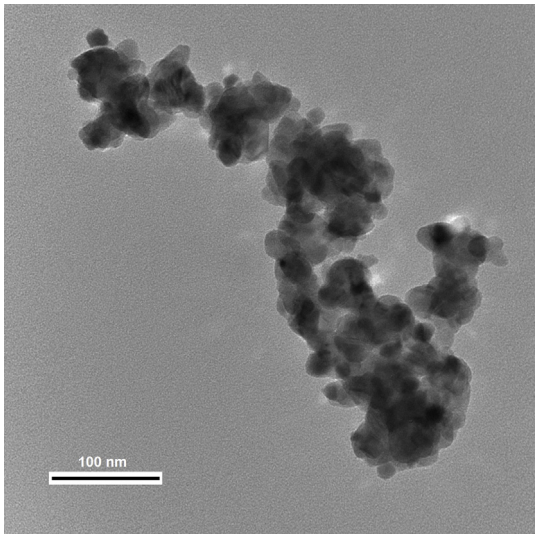

Fig. 4. TEM image of powder prepared by the solid state reaction method at 500 °C.

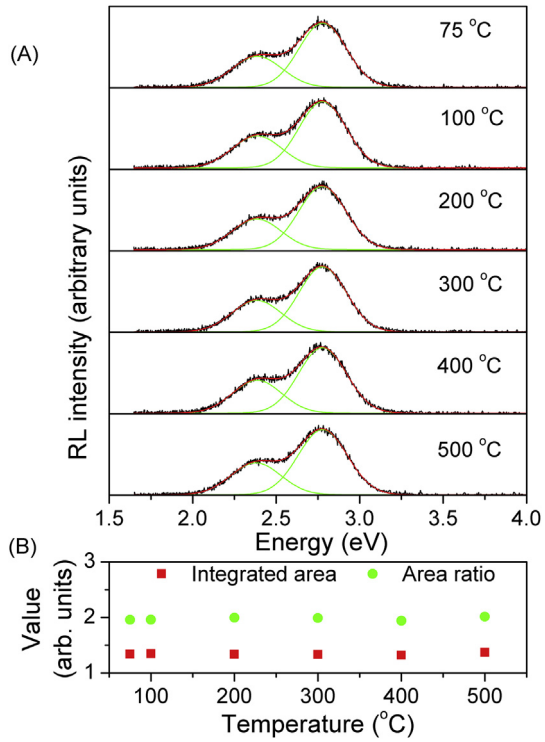

Fig. 5. A) RL spectra of ZnS:Ag prepared with different solid state reaction temperatures (black lines), together with best-fit (red line) based on two Gaussian bands (green lines). B) total integrated area (red squares) and the 2.78/2.38 band area ratio (green circles) as a function of the solid state reaction temperature. (For interpretation of the references to colour in this figure legend, the reader is referred to the Web version of this article.)

prepared at different temperatures. The spectra were composed of a main band centered at 2.78 eV and a shoulder at 2.38 eV, in agreement with previous results of undoped ZnS prepared by solid state reaction [9,10]. The 2.78 eV has been assigned to the donor-acceptor recombination involving a S vacancy (donor) and a Zn vacancy (acceptor) [10,11], while the nature of the 2.38 eV remains elusive. The spectra were analyzed by best-fitting (red line) using two Gaussian bands (green lines). The 2.78/2.38 band area ratio (green circles) and the integrated RL intensity (red squares) were found to remain constant as a

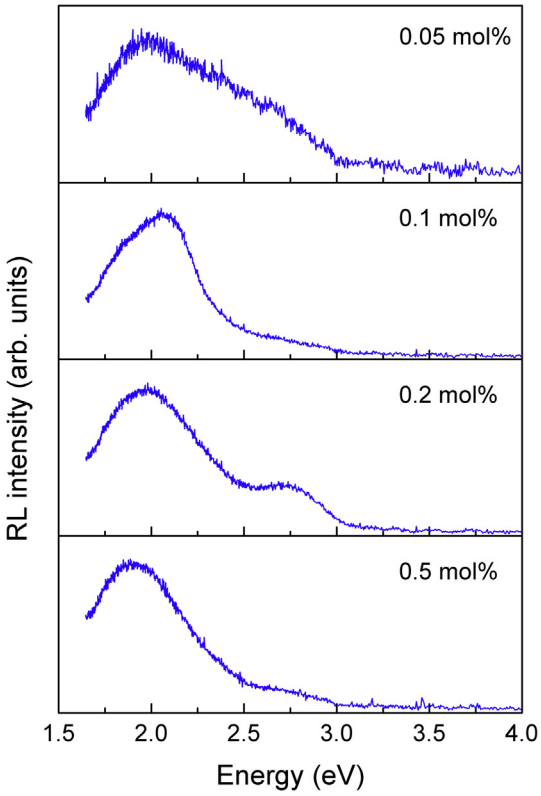

Fig. 6. RL spectra of ZnS:Ag with different Ag concentrations.

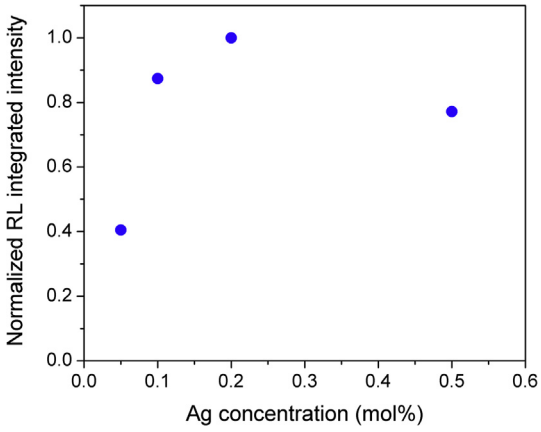

Fig. 7. Normalized integrated RL intensity as a function of the Ag concentration.

function of the solid state reaction temperature (Fig. 5B). These results demonstrated the reaction temperature did not affect the RL output of the host.

In addition to the investigation of the effects of the solid state reaction temperature on the luminescence of the ZnS host, the effects of the incorporation of Ag substituting for Zn was also executed. XRD revealed that the samples with Ag concentrations higher than 0.5 mol% contained a ZnO secondary phase (according to JCPDS no. 36-1457) and were no longer considered in this work. Fig. 6 presents the RL spectra of ZnS powders with different Ag concentrations, namely 0.05, 0.1, 0.2, and 0.5 mol%. Two major bands were observed centered at around 1.95 eV and between *ca.* 2.3 and 3.0 eV. In ZnS:Ag, it is well established that the band centered at about 2.75 eV band is due to electron-hole recombination involving a shallow donor level estimated to be 0.1 eV below the edge of the conduction band [11] and assigned to a sulfur vacancy, and an Ag ion substituting for Zn as the acceptor

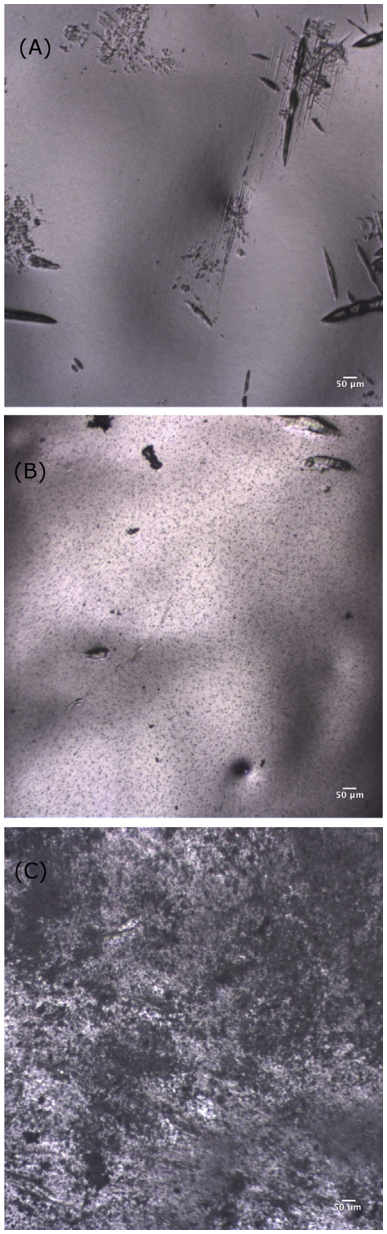

Fig. 8. Optical microscopy images of: A) as-received ultrafiltration membrane, B) surface modified ultrafiltration membrane [1], and C) modified ultrafiltration membrane coated with ZnS:Ag powder. All images were obtained under the same magnification, and the scale bar measures 50 µm.

level [12–14]. The emission around 1.9 eV is also assigned to a shallow donor-deep acceptor recombination, with the recombination center being assigned to a [Ag_{Zn}-D_S] complex, with Ag in its d^9 configuration substituting for Zn and the associate defect D being unidentified [15], though suggested to be a sulfur vacancy [16]. The normalized integrated RL intensity as a function of the Ag concentration showed the RL output of ZnS:Ag was maximized for the Ag concentration of 0.2 mol % (Fig. 7).

The major steps of the fabrication of the ultrafiltration membrane scintillator are illustrated in the optical microscopy images shown in Fig. 8: (A) the as-received ultrafiltration membrane, (B) the surface modified ultrafiltration membrane [1], and (C) of the modified ultrafiltration membrane coated with ZnS:Ag. The presence of ZnS:Ag onto the surface of the modified ultrafiltration membrane was evident by the darkening of the white reflective membrane. Further, the image revealed a homogeneous and nearly complete coverage of the surface.

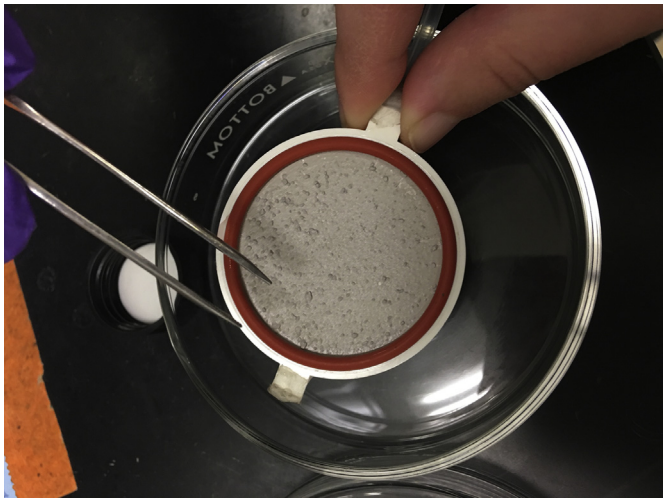

Fig. 9. General aspects of the ultrafiltration membrane scintillator after loading with ZnS:Ag powder.

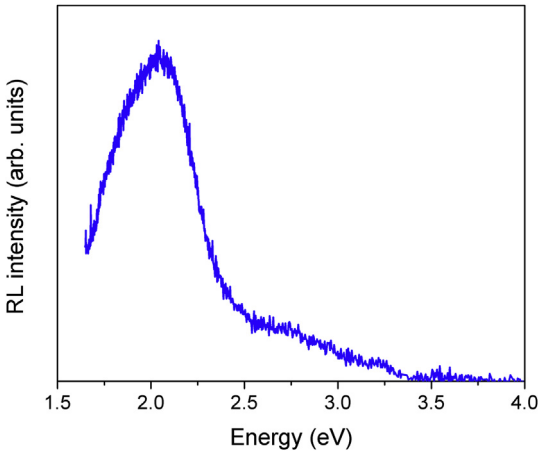

Fig. 10. RL spectrum of the membrane coated with ZnS:0.1 mol% Ag powder prepared by the solid state reaction method.

Fig. 9 shows the general aspects of the ultrafiltration membrane scintillator immediately after the loading of ZnS:Ag powder, where a continuous homogeneous layer of ZnS:Ag powder covering the surface of the modified ultrafiltration membrane can be observed. RL spectroscopy was used to characterize the response the ultrafiltration membrane scintillator under exposure to ionizing radiation, and a typical RL spectrum is shown in Fig. 10. RL emission was dominated by a relatively broad band centered around 2.0 eV, indicating that the fabrication procedure of the membrane scintillator did not affect the luminescent properties of the ZnS:Ag powder and demonstrating the scintillation response of the ultrafiltration membrane scintillator to ionizing radiation.

4. Conclusions

In this work, the fabrication of an ultrafiltration membrane scintillator based on ZnS:Ag was demonstrated. The synthesis of ZnS:Ag was achieved by means of the solid state reaction method, with particular emphasis on the investigation of the effects of the reaction temperature on the ZnS host and of the Ag concentration on the RL output. The reaction temperature was found to control the crystallite size that ranged from 3 to 10 nm, while the RL output was maximized for the Ag concentration of 0.2 mol%. Modified commercial ultrafiltration membranes were coated with ZnS:Ag powder via an ultrafiltration process

and their response to ionizing radiation demonstrated by RL measurements.

Acknowledgements

This work was supported by the Defense Threat Reduction Agency through contract HDTRA 1-16-1-0016.

References

[1] C.E. Duval, A.W. Darge, C. Ruff, T.A. DeVol, S.M. Husson, Anal. Chem. 90 (2018) 4144.
[2] G.F. Knoll, Radiation Detection and Measurement, fourth ed., Wiley, 2010, p. 238.
[3] M. Kobayashi, M. Ishii, W.M. Yen, S. Shionoya, H. Yamamoto (Eds.), Practical Applications of Phosphors, CRC Press, 2007, p. 298.
[4] http://www.emdmillipore.com/US/en/product/Ultrafiltration-Discs-100kDa-NMW,MM_NF-PBHK04310#overview.
[5] The Stopping and Range of Ions in Matter (http://www.srim.org/).
[6] B.D. Cullity, Elements of X-Ray Diffraction, second ed., Addison-Wesley Pub. Co., 1978, p. 284.
[7] L. Wang, X. Xu, X. Yuan, J. Lumin. 130 (2010) 137–140.
[8] M.M.H. Farooqi, R.K. Srivastava, Mater. Sci. Semicond. Process. 20 (2014) 61–67.
[9] M. Jothibas, S.J. Jeyakumar, C. Manoharan, I.K. Punithavathy, P. Praveen, J.P. Richard, J. Mater. Sci. Mater. Electron. 28 (2017) 1889.
[10] Z. Chen, X.X. Li, G. Duc, Q. Yu, Opt. Mater. 36 (2014) 1007–1012.
[11] H. Kukimoto, S. Shionoya, T. Koda, R. Hioki, J. Phys. Chem. Solid. 29 (1968) 935.
[12] K. Era, S. Shionoya, Y. Washizawa, J. Phys. Chem. Solid. 29 (1968) 1827.
[13] K. Era, S. Shionoya, Y. Washizawa, H. Ohmatsu, J. Phys. Chem. Solid. 29 (1968) 1843.
[14] Y. Uehara, J. Chem. Phys. 62 (1975) 2982.
[15] N.R.J. Poolton, J. Phys. C Solid State Phys. 20 (1987) 5867.
[16] J. Dieleman, S.H. deBruin, C.Z. van Doorn, J.H. Haanstra, Philips Res. Rep. 19 (1964) 311.